

Study of the High-Coercivity Material Based on ϵ -Fe₂O₃ Nanoparticles in the Silica Gel Matrix

D. A. Balaev^{a, b}, S. S. Yakushkin^{c, d*}, A. A. Dubrovskii^{a, e},
G. A. Bukhtiyarova^c, K. A. Shaikhutdinov^a, and O. N. Martyanov^{c, d}

^a Kirensky Institute of Physics, Russian Academy of Sciences, Siberian Branch, Krasnoyarsk, 660036 Russia

^b Siberian Federal University, Krasnoyarsk, 660041 Russia

^c Boreskov Institute of Catalysis, Russian Academy of Sciences, Siberian Branch, Novosibirsk, 630090 Russia

^d Novosibirsk State University, Novosibirsk, 630090 Russia

^e International Laboratory of High Magnetic Fields and Low Temperatures, Wroclaw, Poland

*e-mail: stas-yk@catalysis.ru

Received October 30, 2015

Abstract—We report the results of investigations of ϵ -Fe₂O₃ magnetic nanoparticles obtained by incipient wetness impregnation of silica gel. It was established that the obtained samples with an iron content of 12–16% mass % containing ϵ -Fe₂O₃ nanoparticles with an average size of 10 nm on the silica gel surface exhibit a room-temperature coercivity of about 10 kOe. Along with fabrication simplicity, this fact makes the prepared samples promising for application as a magnetically hard material.

DOI: 10.1134/S1063785016040039

The polymorphic modification of trivalent iron oxide ϵ -Fe₂O₃ characterized for the first time in [1] is attracting the attention of researchers, first of all, due to its unique magnetic properties [2], including the magnetic transition in the range of 80–150 K and giant room-temperature coercivity H_C , which reaches ~20 kOe. The latter offers opportunities for use of this oxide as a magnetically hard material.

The ϵ -Fe₂O₃ modification exists only in nanosized form due to the low surface energy of its structure [2–4] consisting of particles with a maximum size of about 25–40 nm [2, 3] in the SiO₂ matrix. As the particle size is increased, transition to a more thermodynamically favorable iron oxide modification, α -Fe₂O₃, occurs [4], which prevents the formation of ϵ -Fe₂O₃ without impurities of other polymorphic modifications.

There exist several approaches to the synthesis of ϵ -Fe₂O₃ nanoparticle systems, which are based mainly on tempering the initial nanoparticles of γ -Fe₂O₃ oxide [1, 5], Fe₃O₄ [6], and even α -Fe₂O₃ [7], or on the temperature treatment of a mesoporous carrier matrix containing ionic precursor compounds [8, 9].

Incipient wetness impregnation with the Fe(II) sulphate solutions with subsequent thermal treatment is a relatively simple technique for obtaining ϵ -Fe₂O₃ nanoparticles in a silica gel matrix [10, 11]. The advantage of this technique, along with its simplicity, is the possibility of forming single-phase ϵ -Fe₂O₃ particles a few nanometers in size, which is much smaller than

the above-mentioned values of 25–40 nm. Upon transition to the nanometer scale, the magnetic properties change, which is of special interest; in addition, small (2–6 nm) ϵ -Fe₂O₃ particles exhibit superparamagnetic behavior [12–15] and, consequently, the room-temperature magnetization curve is hysteresis-less ($H_C = 0$). In [12–15], we studied the samples containing up to ~7 mass % Fe in the form of ϵ -Fe₂O₃ particles deposited onto silica gel. The average ϵ -Fe₂O₃ particle size was ~10 nm; the sample contained also particles with a size of ~20 nm. To enhance the room-temperature coercivity, it is necessary to overcome the superparamagnetic (SP) limit, i.e., increase the SP blocking temperature T_B ($T_B \sim V$, where V is the particle volume). Within the above-mentioned technique for synthesizing ϵ -Fe₂O₃ particles, it can be implemented by an increase in the average particle size, which is attained by multiple impregnations. This Letter presents the results of investigations of the magnetic properties of the ϵ -Fe₂O₃ particles with an iron mass content of up to ~16%.

The synthesis technique involves the following stages: (i) impregnation of ChemAnalyt KSKG silica gel with a specific surface area of 287 m²/g, an average pore radius of ~140 Å, a pore volume of ~0.35 cm³/g, and a grain size of 0.25–0.5 nm with the aqueous solution of Fe(II) sulphate (ACS 99+%, CAS 7782-63-0); (ii) drying at a temperature of 110°C for 4 h; and (iii) annealing in air at a temperature of 900°C for 4 h.

Sample designation (number of impregnations indicated in parentheses), iron content, coercivity, and HRTEM average size

Sample	Fe, mass %	H_C (4.2K), kOe	H_C (290K), kOe	$\langle d \rangle$, nm
05FS(<i>I</i>)	0.74	0.5	0	3.4
3FS(<i>I</i>)	3.4	1.5	1.7	3.8
6FS(<i>I</i>)	5.6	3.9	7.4	~10
12FS(<i>3</i>)	12.5	5.3	8.5	>10
16FS(<i>5</i>)	16.1	7.6	9.4	>10

To increase the iron mass content, the first and second stages were multiply repeated. The Fe mass content in the investigated samples, sample designation, and average particle sizes are given in the table.

High-resolution transmission electron microscopy (HRTEM) images were obtained on a JEOL JEM-2010 microscope operating at 200-kV accelerating voltage and ensuring resolution of up to 1.4 Å. The X-ray diffraction study was carried out using an XTRA powder diffractometer in Cu K_α radiation at a wavelength of $\lambda = 1.5418$ Å, a scanning pitch of 0.050 by 2θ , and a point accumulation time of 3 s. The magnetic measurements were performed on a vibrating sample magnetometer. The data on the magnetic moment were normalized to the Fe_2O_3 mass in the sample.

Figure 1a shows X-ray diffraction patterns of samples 3FS(*I*) and 12FS(*3*) (the designation principle is clear from the table), as well as of the used silica gel

carrier (init). The carrier is characterized by a halo typical of the amorphous state; for samples 3FS(*I*) and 12FS(*3*), one can see reflections belonging to the $\epsilon\text{-Fe}_2\text{O}_3$ phase (corresponding indices hkl are shown). According to the HRTEM data, sample 3FS(*I*) contains mainly particles smaller than 10 nm (average size is ~3.8 nm; see table and Fig. 1b), which leads to strong broadening of diffraction peaks (Fig. 1a) [11, 12]. Samples subjected to two or more impregnations contain mainly the particles over 10 nm in size (Fig. 1b). However, the diffraction pattern of sample 12FS(*3*) contains the hematite peaks. The formation of $\alpha\text{-Fe}_2\text{O}_3$ particles as a phase accompanying $\epsilon\text{-Fe}_2\text{O}_3$ is encountered fairly often during the synthesis [2, 3]. Our estimation shows that the amount of hematite in sample 12FS(*3*) is ~5%. Stages of the formation of the $\epsilon\text{-Fe}_2\text{O}_3$ system and occurrence of the foreign hematite phase will be studied elsewhere.

Figure 2 shows temperature dependences of magnetic moment $M(T)$ for the investigated samples. The $M(T)$ dependence for sample 05FS(*I*) has a maximum at a temperature of ~15 K; below ~35 K, the $M(T)$ dependences measured in the zero-field cooling (ZFC) and field cooling (FC) regimes ($H = 1$ kOe) diverge. As the external field is increased, the described features are observed at lower temperatures. Such a behavior is typical of SP particles. At the same time, the rest samples exhibit the $M(T)$ maximum near 130 K in both the ZFC and FC regime (not shown). In addition, the position of the $M(T)$ maximum for these samples is nearly invariable at the change in the external field to 10 kOe; therefore, the characteristic temperature of ~130 K is not an SP blocking temperature.

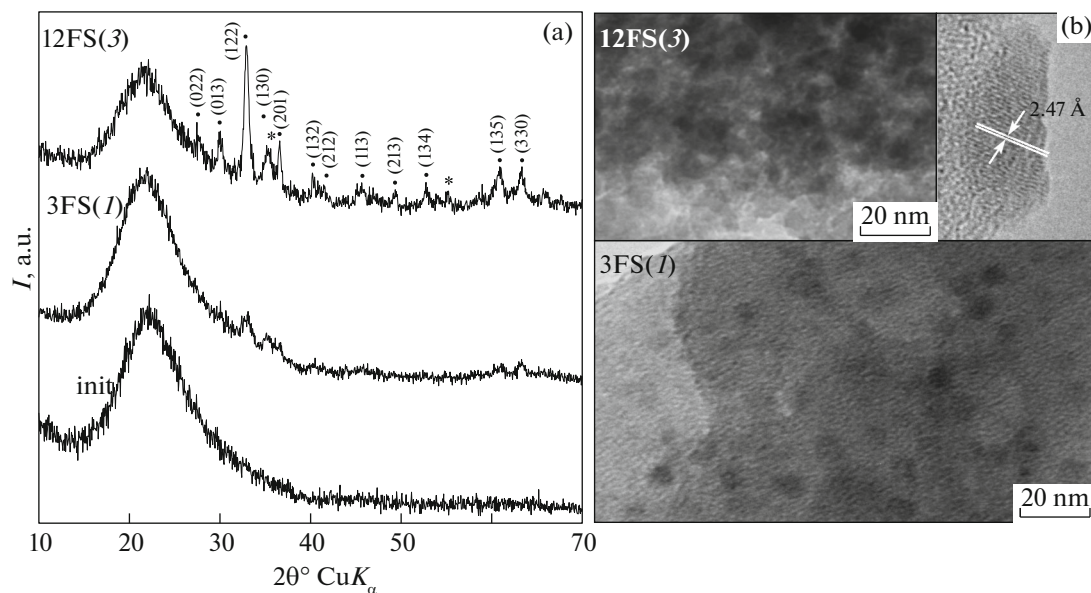


Fig. 1. (a) X-ray diffraction patterns of samples 3FS(*I*) and 12FS(*3*) and initial silica gel (init). Crystal reflections corresponding to the $\epsilon\text{-Fe}_2\text{O}_3$ (•) and $\alpha\text{-Fe}_2\text{O}_3$ (*) phases are indicated. (b) HRTEM images of samples 3FS(*I*) and 12FS(*3*). Inset: image of atomic layers in a $\epsilon\text{-Fe}_2\text{O}_3$ particle in sample 12FS(*3*).

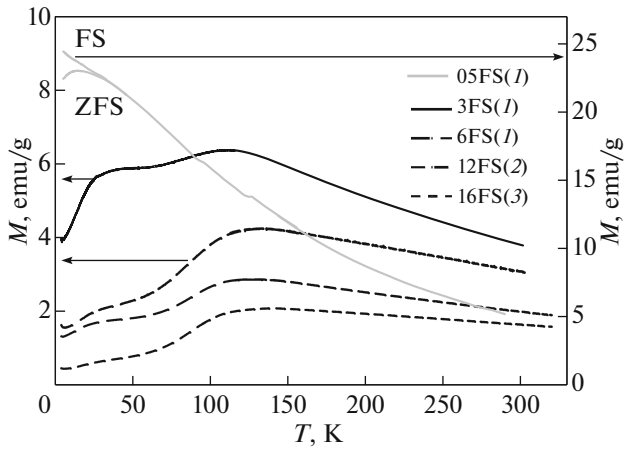


Fig. 2. Temperature dependences of the magnetic moment $M(T)$ for the investigated samples in an external field of $H = 1$ kOe obtained in the zero-field cooling (ZFC) and field cooling (FC) regimes. For sample 05FS(I), data on the FC conditions are also presented (M axis, right scale).

Most particles in the samples with an iron content over 3% are blocked up to room temperature. The discussed nonmonotonic behavior of the $M(T)$ dependences is related to the magnetic transition to ϵ - Fe_2O_3 that occurs in the range of 80–150 K [2, 3, 16, 17]. The transition of small particles to the blocked state in the low-temperature region (below ~ 80 K), as for sample 05FS(I), is revealed in the $M(T)$ dependences as a plateau (Fig. 2).

Figure 3 shows magnetization curves $M(H)$ for the investigated samples at $T = 290$ K. Since, at room temperature, all particles in sample 05FS(I) are in the SP state (Fig. 2), the $M(H)$ dependence is completely reversible. The $M(H)$ dependences of the rest of the samples are hysteretic. As the iron content in the samples is increased, the coercivity grows (see Fig. 3 and table). This is related to an increase in the ϵ - Fe_2O_3 particle size. For sufficiently large particles, the hysteresis behavior is observed, whereas the particles in the unblocked state ($T > T_B$) contribute to the integral hysteresis loop of the entire sample, similar to the $M(H)$ dependence for sample 05FS(I). This significantly modifies the $M(H)$ dependence, which is sufficiently narrow near the origin of coordinates (this is the most pronounced for sample 3FS(I)), and leads to a decrease in the H_C values of the entire sample. In addition, at the retained single-domain state of particles, which is valid for ϵ - Fe_2O_3 up to a size of 25 nm [16], the coercivity also increases with size. The afore-said explains the observed variation in the H_C value of the investigated samples with increasing ϵ - Fe_2O_3 nanoparticle size. The data at $T = 4.2$ K (see table) confirm the described H_C behavior.

The largest room-temperature coercivity $H_C \approx 9.4$ kOe was obtained for sample 16FS(5) and is

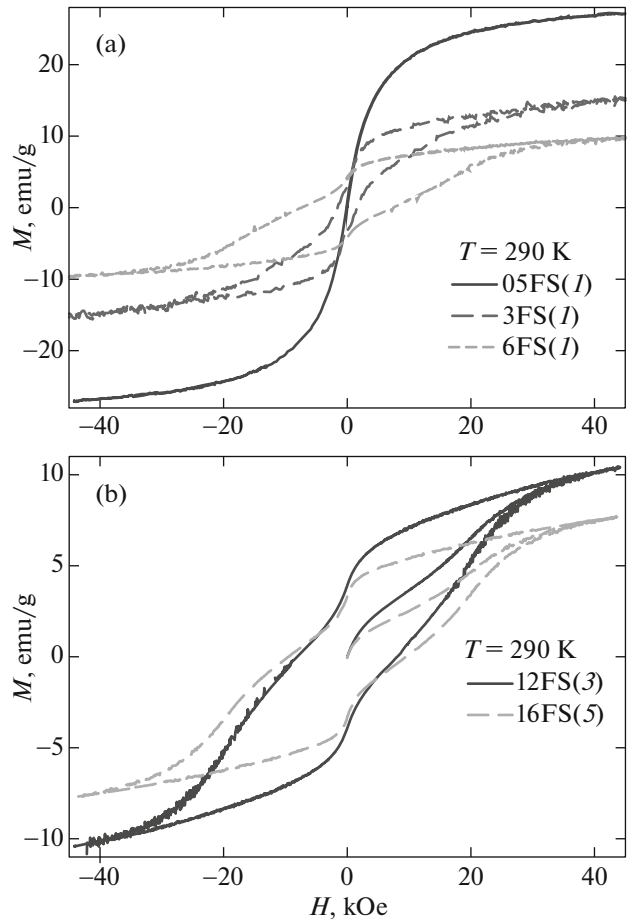


Fig. 3. Magnetic hysteresis loops observed in the investigated ϵ - Fe_2O_3 samples.

apparently close to the maximum value for the samples obtained by multiple impregnations. At high iron contents in the samples, the main part of the oxide phase is α - Fe_2O_3 . Consequently, we can say that there is an optimal iron content of 12–16 mass % in the samples at which the particles become larger than after one impregnation, the fraction of small (< 8 nm) particles decreases, the amount of the foreign hematite phase is small, and the room-temperature coercivity is about 9 kOe.

Thus, the investigated samples exhibit the formation of ϵ - Fe_2O_3 nanoparticles with a characteristic size of more than 10 nm and a coercivity of ~ 9 kOe, which is the maximum value for ϵ - Fe_2O_3 particles of this size. Owing to the relative simplicity and low cost of the proposed silica gel impregnation technique, the obtained material is promising for application as a magnetically hard material.

Acknowledgments. We are grateful to M.A. Kazakova for her help in sample preparation.

This study was supported by the Federal Agency for Scientific Organizations of Russia (base budget

financing no. V.44.1.15), the Scientific and Educational Center of Energy-Efficient Catalysis at the Novosibirsk State University, and the Russian Foundation for Basic Research (project no. 15-32-50919).

REFERENCES

1. E. Tronc, C. Chaneac, and J. P. Jolivet, *J. Solid State Chem.* **139** (1), 93 (1998).
2. L. Machala, J. Tucek, and R. Zboril, *Chem. Mater.* **23**, 3255 (2011).
3. J. Tucek, R. Zboril, A. Namai, and S. Ohkoshi, *Chem. Mater.* **22**, 6483 (2010).
4. S. Ohkoshi, S. Sakurai, J. Jin, and K. Hashimoto, *J. Appl. Phys.* **97**, K312 (2005).
5. R. Zboril, M. Mashlan, K. Barcova, and M. Vujtek, *Hyperfine Interact.* **139/140**, 597 (2002).
6. Y. Ding, J. R. Morber, R. L. Snyder, and Z. L. Wang, *Adv. Funct. Mater.* **17** (7), 1172 (2007).
7. M. Tadic, V. Spasojevic, V. Kusigerski, D. Markovic, and M. Remskar, *Scr. Mater.* **58** (8), 703 (2008).
8. M. Popovici, M. Gich, D. Niansk, et al., *Chem. Mater.* **16** (25), 5542 (2004).
9. S. Sakurai, J. Shimoyama, K. Hashimoto, and S. Ohkoshi, *Chem. Phys. Lett.* **458**, 333 (2008).
10. G. A. Bukhtiyarova, O. N. Mart'yanov, S. S. Yakushkin, M. A. Shuvaeva, and O. A. Bayukov, *Phys. Solid State* **52** (4), 826 (2010).
11. G. A. Bukhtiyarova, M. A. Shuvaeva, O. A. Bayukov, S. S. Yakushkin, and O. N. Martyanov, *J. Nanopart. Res.* **13** (10), 5527 (2011).
12. S. S. Yakushkin, A. A. Dubrovskiy, D. A. Balaev, K. A. Shaykhutdinov, G. A. Bukhtiyarova, and O. N. Martyanov, *J. Appl. Phys.* **111** (4), 044312 (2012).
13. S. S. Yakushkin, G. A. Bukhtiyarova, and O. N. Mart'yanov, *J. Struc. Chem.* **54** (5), 876 (2013).
14. D. A. Balaev, A. A. Dubrovskiy, K. A. Shaykhutdinov, O. A. Bayukov, S. S. Yakushkin, G. A. Bukhtiyarova, and O. N. Martyanov, *J. Appl. Phys.* **114**, 163911 (2013).
15. I. S. Poperechny, A. A. Krasikov, K. A. Shaikhutdinov, A. A. Dubrovskiy, S. I. Popkov, A. D. Balaev, S. S. Yakushkin, G. A. Bukhtiyarova, O. N. Martyanov, and Yu. L. Raikher, *J. Appl. Phys.* **117**, 063908 (2015).
16. M. Gich, A. Roig, C. Frontera, E. Molins, J. Sort, M. Popovici, G. Chouteau, D. Martin, Y. Marero, and J. Nogues, *J. Appl. Phys.* **98** (4), 044307 (2005).
17. M. Kurmoo, J.-L. Rehspringer, and A. Hutlova, *Chem. Mater.* **17**, 1106 (2005).

Translated by E. Bondareva